HHS Public Access

Author manuscript

J Clin Neurophysiol. Author manuscript; available in PMC 2022 September 01.

Published in final edited form as:

J Clin Neurophysiol. 2021 September 01; 38(5): 366–375. doi:10.1097/WNP.0000000000000719.

Do Triphasic waves and Non-Convulsive Status Epilepticus arise from similar mechanisms? A computational model

Sophie Ligtenstein, MS[1], **Jiangling Song, PhD**[2], **Jin Jin, PhD**[3], **Haoqi Sun, PhD**[3], **Luis Paixao, MD**[3], **Sahar Zafar, MD**[3], **M. Brandon Westover, MD, PhD**[3,*]

[1]Department of Technical Medicine, Department of Applied Mathematics, University of Twente

[2]Northwest University, Xi'an, China

[3]Department of Neurology, Massachusetts General Hospital, Boston MA

Abstract

Background—Triphasic waves (TW) arising in patients with Toxic Metabolic Encephalopathy (TME), are often considered different from generalized periodic discharges (GPDs) in patients with Generalized Non-Convulsive Status Epilepticus (GNCSE).

Objectives—The primary objective of this study is to investigate whether a common mechanism can explain key aspects of both TWs in TME and GPDs in GNCSE.

Method—We used a neural mass model for the simulation of EEG patterns in patients with Acute Hepatic Encephalopathy (AHE), a common etiology of TME. Increased neuronal excitability and impaired synaptic transmission due to elevated ammonia levels in AHE patients were used to explain how TWs and GNCSE arise. We also studied the effect of gamma-aminobutyric acid (GABA)-ergic drugs on epileptiform activity, simulated with a prolonged duration of the inhibitory postsynaptic potential.

Main results—The simulations show that a model which includes increased neuronal excitability and impaired synaptic transmission can account for both the emergence of GPDs and GNCSE and their suppression by GABA-ergic drugs.

Conclusion—Our results add to evidence from other studies calling into question the dichotomy between TWs in TME and GPDs in GNCSE, and support the hypothesis that all GPDs, including those arising in TME patients, occur via a common mechanism.

Keywords

Toxic Metabolic Encephalopathy; generalized periodic discharges; triphasic waves; mean field model; electroencephalography

[*]Corresponding author: M. Brandon Westover, MD, PhD, Massachusetts General Hospital, Neurology Department, 55 Fruit Street, Boston, MA, 02114, FAX: 617-726-3311, mwestover@mgh.harvard.edu.

1 Introduction

Toxic Metabolic Encephalopathy (TME) is an acute condition of generalized depression of cerebral function, induced by an exogenous or endogenous disturbance of the central nervous system's normal chemical milieu (1; 2). TME is common among patients with critical illness who are admitted to an Intensive Care Unit (ICU) (3). The clinical presentation of TME varies from mild confusion and cognitive slowing ('delirium') to stupor or coma (4).

The electroencephalogram (EEG) of patients with TME can be characterized by the appearance of generalized periodic discharges (GPDs). These discharges are often referred to as 'triphasic waves' (TWs), but more recently have been formalized in the newer nomenclature of the ACNS as Generalized Periodic Discharges with Triphasic morphology. Features that have been proposed for GPDs to qualify as TWs include an amplitude between 100 and 300 μV, a frequency of 1.0 – 2.0 Hz, a negative-positive-negative phase polarity, an anterior-to-posterior phase lag, and responsiveness to state changes or stimulation (6; 7).

A distinction is often made between the TWs in TME and GPDs occurring in patients with Generalized Non-Convulsive Status Epilepticus (GNCSE). While TWs are generally not regarded as a type of seizure activity, GPDs arising in GNCSE are (8; 9). In 2006, Boulanger et al. described morphological features which they claimed can distinguish the two types of discharges, and reported that TWs were more responsive than GPDs to noxious or auditory stimulation (9). Furthermore, it is common to administer anti-seizure drugs (ASDs) to patients diagnosed with GNCSE consisting of GPD patterns, but to withhold ASDs from patients diagnosed with TME who exhibit TWs.

Recent studies and a careful reading of prior literature suggest that the above mentioned differences may not robustly distinguish TWs from other GPDs. First, in the study of Boulanger et al., there is overlap in the etiologies they assigned to the TW group and the GPD group; and it is now well established that medical conditions leading to encephalopathy (e.g. renal failure, liver failure, drug toxicity, etc) can produce unequivocal clinical and electrographic seizures [REF]. Furthermore, in Boulanger et al., classification of periodic discharges as TWs vs GPDs was based on review by only two EEG reviewers, whereas a recent study of Foreman et al. showed that the inter-rater agreement for making this distinction is only 33%. The study of Foreman et al. also showed that some TWs were associated with development of seizures (10). Finally, recent evidence suggests that a proportion (~40%) of patients with TWs show clinical improvement after treatment with ASDs (6; 10).

The conceptual division between GPDs in TME and GNCSE is important, because treatment recommendations depend on whether this distinction is artificial vs fundamental. Herein we propose a theory to unify several recent observations. We propose that GPDs in the setting of TME are a (usually) mild form of seizure activity that occur via the same underlying mechanisms as GPDs in GNCSE. In our theory, mild TME leads to the GPDs conventionally described as TWs, while severe TME leads to GPDs seen in NCSE. We investigate this

theory using a computational model for simulating GPDs arising in one of the best described forms of TME, Acute Hepatic Encephalopathy (AHE).

AHE is a common etiology for TME and can occur as a result of acute liver failure or an acute exacerbation of chronic liver failure (11). The syndrome is potentially reversible and its clinical presentation depends on the severity of the disease as shown in Table 1 (7; 12; 13; 14; 15). TWs arise in more severe grades of AHE.

We use a recently-proposed mean field model of GPDs arising in AHE to gain insight into the pathophysiological mechanisms leading to the emergence of TWs and their response to ASDs (16). This prior work shows how a biologically plausible mathematical model that incorporates elevated neuronal excitability and impaired synaptic transmission, key features of AHE arising from known pathophysiological mechanisms, can give rise to GPDs/TWs. We review the model here, and study in depth the responsiveness of the model to gamma aminobutyric acid (GABA)-ergic ASDs, comparing the model responses with known effects of ASDs on GPDs/TWs. The primary objective of this study is to investigate the output of the neural mass model and the potential corresponding clinical implications, in support of the view that the distinction between TWs in TME and GPDs in GNCSE is ultimately an artificial one.

2 Methods

2.1 Background of neural mass model

We use a previously published neural mass model of GPDs arising in AHE (16). Mathematical details are provided in the Supplemental Material. Our model is based on a modified Liley model developed by Ruijter et al. to explain the appearance of GPDs in patients with hypoxic-ischemic encephalopathy (HIE) (17). In (16), the model was adapted to study AHE by mapping the mechanisms included in the model onto pathophysiological mechanisms described in the literature on AHE. Figure 1 shows an overview of the computational model, consisting of one excitatory population, the pyramidal neurons, and one inhibitory population, the inter-neurons. The brain involves both cortical and subcortical sources. In the model, cortical sources are represented by sigmoid activation functions as shown in Figure 2A. The figure shows how the membrane potential influences the rate of neuronal firing. Subcortical (thalamic) sources are both excitatory. We model p_{ei} as a constant and p_{ee} as a constant plus whitenoise.

Calculation of the postsynaptic potential (PSP) is as follows. The presynaptic potential is transformed into a mean firing rate using the sigmoid activation function. Filtering of this firing rate by the synaptic response function results in the PSP, displayed in Figures 2B and 2C. The output of the model is a simulated EEG signal, based on the inverse of the mean excitatory soma membrane potential $V_e(t)$. All model computations were executed with Matlab (Matlab R2018a, Mathworks Inc., Natick, Massachusetts, USA). The model equations and parameters are further explained in Appendix A.

2.2 AHE-specific adaptions to model

Increased neuronal excitability in patients with AHE is thought to result from multiple causes. One key cause is an up to ten-fold increased level of NH_3, which can result in excessive activation of N-methyl-D-asparate (NMDA) type glutamate receptors leading to elevated neuronal excitability (18; 19). This can be modeled by increasing the resting value of the maximum excitatory postsynaptic potential (EPSP) amplitude (Γ^{rest}_e). We implement this in the model by changing the amplification factor F_{am}. An increased F_{am} corresponds to an increased excitatory postsynaptic potential, as shown in Figure 2B.

Alterations in NH_3 levels can also lead to reduction in brain concentrations of adenosine triphosphate (ATP) (18). ATP levels are also decreased due to elevated consumption resulting from increased activity of the Na^+-K^+-ATPase in patients with AHE (20). Decreased levels of ATP eventually lead to impaired synaptic transmission. This is modeled by adjusting postsynaptic peak amplitudes Γ_e and Γ_i, which correspond to the maximum values of the synaptic response functions shown in Figures 2B and 2C. These amplitudes are considered as variables dependent on the presynaptic firing rate and recovery time constant τ_e^{rec} and τ_i^{rec}, respectively. Simulations were performed with varying values of the two time constants.

2.3 Effect of GABA-ergic drugs

Figure 2C shows how we model the effect of administration of GABA-ergic drugs, leading to prolongation of the inhibitory postsynaptic potential (IPSP). This can result in suppression of GPDs and seizures (6). We modeled this effect by adjusting the decay rate constants γ_i and $\tilde{\gamma}_i$. These constants can be adapted by changing parameter c, which will be referred to as GABA in this paper.

2.4 Categorization of simulated EEG signals

Simulated EEG signals are categorized into one of the nine categories using an automated method, following criteria outlined in Figure 3. The nine categories are: no discharges, burst-suppression, irregular discharges, periodic discharges (<1 Hz), periodic discharges (1 – 1.5 Hz), periodic discharges (1.5 – 2 Hz), periodic discharges (2 – 2.5 Hz), periodic discharges (2.5 – 3 Hz) and seizures (>3 Hz) (21). An example of each pattern category, generated by the model, is shown in Figure 4. It should be kept in mind that the voltages of the simulated EEG signals do not correspond to those of real EEG signals.

2.5 Simulations

We conducted 16 simulations, in groups of 4. In these simulations we varied four parameters which govern model behavior: F_{am}, representing the degree of increased neuronal excitability; τ_i^{rec} and τ_e^{rec}, the inhibitory interneuron and excitatory neuron synaptic recovery times, representing the degree of impairment of synaptic transmission; and GABA, the level of GABA-ergic drug in the CNS (e.g. due to administration of benzodiazepine drugs). In each of the 4 groups of 4 simulations, we choose two of the 4 parameters to vary continuously along the x and y axis of a subfigure. We generate 4 subfigures by selecting two levels for the other two parameters, and using one of these levels for the figures in the top row, and the other value for the figures in the bottom row. We repeat

this for the other parameter, using one value for the figures in the left column and the other for figures in the right column. In this way, each group of experiments generates 4 figures in a 2×2 configuration.

In each subfigure the type of activity generated by the model is indicated by the colors shown in Figure 3. The colors are organized such that increasingly deeper shades of red indicate periodic discharges of increasing frequencies, with seizures (periodic discharges at >3Hz) indicated by the darkest shade of red. Burst suppression is indicated by orange, irregular or sporadic discharges by yellow, and patterns without burst suppression or discharges, by green.

In all plots, we only show regions of the parameter space where excitatory synaptic transmission is more severely impaired than inhibitory synaptic transmission; that is, we show only regions where the recovery time for excitatory EPSPs τ_e^{rec} is elevated to a greater degree than the recovery time for inhibitory EPSPs τ_i^{rec} (i.e. $\tau_e^{rec} > \tau_i^{rec}$. Regions where this is not true were considered physiologically implausible (17) and are therefore shaded out in the figures.

Clinically relevant values for GABA, F_{am}, τ_e^{rec} and τ_i^{rec} were estimated in a prior study (16). An overview of the values is given in Table 2.

3 Results

3.1 Simulations

The results of simulations are presented in Figures 5, 6, 7 and 8. Each plot focuses on how model behavior changes depending on a different combination of model parameters that govern neuronal excitability and synaptic neurotransmission. Figure 4 provides examples of the nine pattern types that we defined to categorize simulated EEG activity, along with a key to the colors used in the figures.

Figure 5 shows how EEG activity produced by the model varies depending on the major factors that are impaired in AHE. Each of the four panels shows the type of neuronal activity produced by the model, depending on the degree of impaired synaptic transmission (i.e. the degree to which excitatory and inhibitory EPSP recovery time constants, τ_e^{rec}, τ_i^{rec}, are elevated, e.g. due to reduced ATP levels). The panels differ by the degree of increased neuronal excitability (i.e. the degree to which F_{am} is increased, e.g. due to increased activation of NMDA type glutamate receptors), with models in the left column set to a low value (0.75), and those in the right column set to a high value (1.5). The effects of GABA-ergic medication are also shown, with upper panels indicating no treatment (GABA = 0), and lower panels indicating treatment (GABA = 0.1). We make three observations. First, the propensity for high frequency periodic discharges (PDs) and seizures increases as neuronal excitability increases, as indicated by the increased proportion of the figures occupied by darker reds when F_{am} is increased (compare right hand panels with left hand panels). Second, treatment generally decreases the burden of high frequency PDs and seizures, as indicated by the decreased proportion of the figures occupied by darker reds when $GABA$ is increased (compare bottom panels with top panels). Third, impaired inhibitory

synaptic transmission (increased τ_i^{rec}; y-axis) leads to increased frequency of discharges, and ultimately to seizures, whereas impaired excitatory synaptic transmission (increased τ_i^{rec}; xaxis) has the opposite effect. The balance between τ_i^{rec} and τ_e^{rec} determines model behavior.

Figure 6 explores in more detail the effects of treatment with GABA-ergic drugs. In each subfigure, GABA-ergic drug levels vary along the x-axis, and the degree of impaired inhibitory synaptic neurotransmission (τ_i^{rec}) varies along the y-axis. The columns again show conditions of lower (left two figures) vs higher (right two figures) levels of neuronal excitability (F_{am}). The rows show conditions of higher (bottom two figures) vs lower (upper two figures) levels of impaired excitatory neuronal synaptic transmission (τ_e^{rec}). Note that large values of τ_e^{rec} indicate more profound dysfunction. We make three observations: First and second, as we saw in the previous figure, increased neuronal excitability (right panels) and increasing impairment of inhibitory neurotransmission (increased values along the yaxis) lead to high frequency PDs and seizures. Third, for any given levels of the other parameters, administration of a GABA-ergic drug is able to abolish seizures, decrease the frequency PDs, and ultimately abolish PDs. However, with more severe pathology (higher values of F_{am}, τ_i^{rec}, or both), higher doses of GABA-ergic drug are required to abolish epileptiform activity.

Figure 7 explores in more detail the effects of increased neuronal excitability, F_{am}. In each subfigure, excitability F_{am} increases along the x-axis, and the degree of impaired inhibitory synaptic neurotransmission τ_i^{rec} varies along the y-axis. The columns again show conditions of lower (left two figures) vs higher (right two figures) levels of GABA-ergic drug. The rows show conditions of higher (bottom two figures) vs lower (upper two figures) levels of impaired excitatory neuronal synaptic transmission (τ_e^{rec}; large values of τ_e^{rec} indicate more profound impairment). We make three observations: First and second, as before we see that the burden of high frequency PDs and seizures is increased by increasing neuronal excitability F_{am}, and by increasingly impaired inhibitory synaptic neurotransmission τ_i^{rec} relative to the degree of impairment of excitatory neurotransmission. Third, for any given values of the other parameters, administration of GABA-ergic drug is able to reduce the frequency of and ultimately abolish epileptiform activity. As before, more severe pathology (higher values of F_{am}, τ_i^{rec}, or both), requires higher doses of GABA-ergic drug to abolish epileptiform activity.

Figure 8 provides more detail about the effects of GABA-ergic drug treatment in relation to increased neuronal excitability. In each subfigure, GABA-ergic drug levels increase along the x-axis, and the degree of increased excitability F_{am} increases along the y-axis. The columns show conditions of lower (left two figures) vs higher (right two figures) levels of impairment of inhibitory neurotransmission (τ_i^{rec}), and the rows show conditions of higher (bottom two figures) vs lower (upper two figures) levels of impaired excitatory neuronal synaptic transmission (τ_e^{rec}), where large values indicate more profound impairment. We make three observations: First and second, as before we see that the burden of high frequency PDs and seizures is increased by increasing neuronal excitability F_{am}, decreased by the level of GABA-ergic drug. Third, increasingly impaired inhibitory synaptic neurotransmission τ_i^{rec} increases the burden of epileptiform activity. Fourth, the burden

of epileptiform activity is higher when the excitatory neurotransmission is less impaired relative to inhibitory neurotransmission.

Finally, in Figure 9 we compare the qualitative response of the model administration of a GABA-ergic drug with the response of a typical patient with GPDs in the setting of TME. We see that, following a bolus administration of lorazepam, as CNS levels of the drug rise, the frequency of GPDs decreases, and finally they resolve. The model exhibits the same qualitative behavior.

4 Discussion

Our results show that a biologically plausible neural computational model of toxic metabolic encephalopathy is able to simulate TWs and nonconvulsive status epilepticus EEG patterns, and the effects of GABA-ergic drugs. These results support the view that TW and NCSE EEG patterns in patients with toxic metabolic encephalopathy are produced by similar mechanisms, differing in severity but not in kind.

4.1 Clinical implications of simulations

These results suggest that a small increase in the severity of the inciting metabolic disturbance (NH_3 levels in our model of AHE) may result in a moderate elevation of neuronal excitability and in moderate synaptic failure, leading to the occurrence of low frequency GPDs/TWs. Higher levels of the inciting metabolic disturbance have a more severe influence on both the neuronal excitability and synaptic transmission, resulting in the onset of high frequency GPDs, consistent with accepted definitions of electrographic seizures. We note that the same underlying mathematical model has been succesfully used to provide an explanation of GPDs arising in the setting of hypoxic ischemic encephalopathy. The primary difference between our model of AHE and the prior model of HIE is the account that we propose for how increased neuronal excitability and impaired synaptic transmission arise in these two different disease processes. As mentioned above, and as argued by others (17), these mechanisms appear quite generic, and are likely involved in some form in most or all conditions giving rise to GPD type EEG patterns. Further supporting the biological plausibility of our model, comparison of the simulated to real EEG responses of GPDs to administration of Lorazepam shows that the model predicts the effect of GABA-ergic drugs correctly. These results, coupled with prior empirical data (6), support the concept of empirical ‘ASD trials’ in patients with periodic discharges in AHE and other forms of TME with ASDs. Nevertheless, ASD trials are not without risk, particularly when using GABA-ergic agents like benzodiazepines. Therefore, the optimal way to select patients with TME and GPDs for ASD trials, and the optimal agent and dose, are important topics for further investigation.

4.2 Limitations

Our model is relatively simple. For example, we did not attempt to model spatial aspects of GPDs. Nevertheless, TWs in AHE patients may often possess interesting spatial characteristics, e.g. an anterior-posterior phase-lag. Spatiotemporal modeling of GPDs is an important topic for future research.

Our modeling efforts in this work focus on GPDs arising in patients with AHE. Numerous other causes of TME are also accompanied by GPDs. We chose to focus on AHE because it is a 'classic' cause of TWs in TME, and because it's underlying pathophysiology is relatively well understood. Nevertheless, the underlying mechanisms generating epileptiform activity in our model (increased neuronal excitability and impaired synaptic transmission) are quite general, and seem likely to be common to many or all forms of TME. (16; 17)

5 Conclusion

A biologically plausible neural computational model was used to simulate increased neuronal excitability and impaired synaptic transmission arising in the setting of toxic metabolic encephalopathy. The model was able to generate periodic discharges and seizures, depending on the severity of the underlying metabolic disturbance, and to recapitulate the effects of GABA-ergic drugs on the EEG. These modeling results strengthen the growing case that triphasic waves arise from similar mechanisms and are thus not fundamentally different from other forms of generalized periodic discharges.

Supplementary Material

Refer to Web version on PubMed Central for supplementary material.

Disclosures of conflicts of Interest and Funding Sources

HS was supported by a Developmental Award from the Harvard University Center for AIDS Research (HU CFAR NIH/NIAID fund 5P30AI060354-16). MBW was supported by the Glenn Foundation for Medical Research and the American Federation for Aging Research through a Breakthroughs in Gerontology Grant; through the American Academy of Sleep Medicine through an AASM Foundation Strategic Research Award; from the Department of Defense through a subcontract from Moberg ICU Solutions, Inc, and by grants from the NIH (1R01NS102190, 1R01NS102574, 1R01NS107291, 1RF1AG064312). MBW is a co-founder of Beacon Biosignals, Inc. Other co-authors report not disclosures.

References

[1]. Angel MJ, Young GB (2011) Metabolic encephalopathies. Neurologic clinics 29(4):837–882. [PubMed: 22032664] –

[2]. Kaufman DM, Geyer HL, Milstein MJ (2016) Delirium/toxic-metabolic encephalopathy in Kaufman's Clinical Neurology for Psychiatrists E-Book. (Elsevier Health Sciences), pp. 129–131.

[3]. McNicoll L, et al. (2003) Delirium in the intensive care unit: occurrence and clinical course in older patients. Journal of the American Geriatrics Society 51(5):591–598. [PubMed: 12752832]

[4]. Plum F, Posner J (1980) Multifocal, diffuse, and metabolic brain diseases causing delirium, stupor, or coma in The diagnosis of stupor and coma. (F.A. Davis Company; 4th Edition edition), pp. 179–296.

[5]. Park KM, et al. (2014) Significance of triphasic waves in metabolic encephalopathy. Korean Journal of Clinical Neurophysiology 16(1):15–20.

[6]. O'Rourke D, et al. (2016) Response rates to anticonvulsant trials in patients with triphasic-wave eeg patterns of uncertain significance. Neurocritical care 24(2):233–239. [PubMed: 26013921]

[7]. Kaplan PW (2004) The eeg in metabolic encephalopathy and coma. Journal of clinical neurophysiology 21(5):307–318. [PubMed: 15592005]

[8]. Foreman B, et al. (2012) Generalized periodic discharges in the critically ill: a case-control study of 200 patients. Neurology 79(19):1951–1960. [PubMed: 23035068]

[9]. Boulanger JM, Deacon C, Lécuyer D, Gosselin S, Reiher J (2006) Triphasic waves versus nonconvulsive status epilepticus: Eeg distinction. Canadian journal of neurological sciences 33(2):175–180.

[10]. Foreman B, et al. (2016) Generalized periodic discharges and 'triphasic waves': A blinded evaluation of inter-rater agreement and clinical significance. Clinical Neurophysiology 127(2):1073–1080. [PubMed: 26294138]

[11]. Frontera JA (2012) Metabolic encephalopathies in the critical care unit. CONTINUUM: Lifelong Learning in Neurology 18(3, Critical Care Neurology):611–639. [PubMed: 22810252]

[12]. Squires RH (2008) Acute liver failure in children in Seminars in liver disease.(© Thieme Medical Publishers), Vol. 28, pp. 153–166. [PubMed: 18452115]

[13]. Foris L, Bhimji S (2018) Encephalopathy, hepatic. StatPearls [Internet]. Treasure Island (FL) [Updated 2018 Sep 12].

[14]. Blei AT, Cordoba J, of the American College of Gastroenterology PPC, ,´ et al. (2001) Hepatic encephalopathy. The American journal of gastroenterology 96(7):1968–1976. [PubMed: 11467622]

[15]. Nabi E, Bajaj JS (2014) Useful tests for hepatic encephalopathy in clinical practice. Current gastroenterology reports 16(1):362. [PubMed: 24357348]

[16]. Song JL, et al. (2019) A novel neural computational model of generalized periodic discharges in acute hepatic encephalopathy. Journal of computational neuroscience 47(2–3):109–124. [PubMed: 31506807]

[17]. Ruijter BJ, Hofmeijer J, Meijer HGE, van Putten MJAM (2017) Synaptic damage underlies eeg abnormalities in postanoxic encephalopathy: A computational study. Clinical neurophysiology 128(9):1682–1695. [PubMed: 28753456]

[18]. Perazzo JC, et al. (2012) Hepatic encephalopathy: An approach to its multiple pathophysiological features. World journal of hepatology 4(3):50. [PubMed: 22489256]

[19]. Auron A, Brophy PD (2012) Hyperammonemia in review: pathophysiology, diagnosis, and treatment. Pediatric nephrology 27(2):207–222. [PubMed: 21431427]

[20]. Rao KVR, Norenberg MD (2012) Brain energy metabolism and mitochondrial dysfunction in acute and chronic hepatic encephalopathy. Neurochemistry international 60(7):697–706. [PubMed: 21989389]

[21]. Chong DJ, Hirsch LJ (2005) Which eeg patterns warrant treatment in the critically ill? reviewing the evidence for treatment of periodic epileptiform discharges and related patterns. Journal of Clinical Neurophysiology 22(2):79–91. [PubMed: 15805807]

[22]. Ermentrout GB, Terman DH (2010) The hodgkin-huxley equations in Mathematical foundations of neuroscience. (Springer Science & Business Media), pp. 9–38.

[23]. Coombes S, beim Graben P, Potthast R, Wright J (2014) Neural fields: theory and applications. (Springer).

[24]. Steyn-Ross A, Steyn-Ross M (2010) Modeling phase transitions in the brain. (Springer).

[25]. Frascoli F, Van Veen L, Bojak I, Liley DT (2011) Metabifurcation analysis of a mean field model of the cortex. Physica D: Nonlinear Phenomena 240(11):949–962.

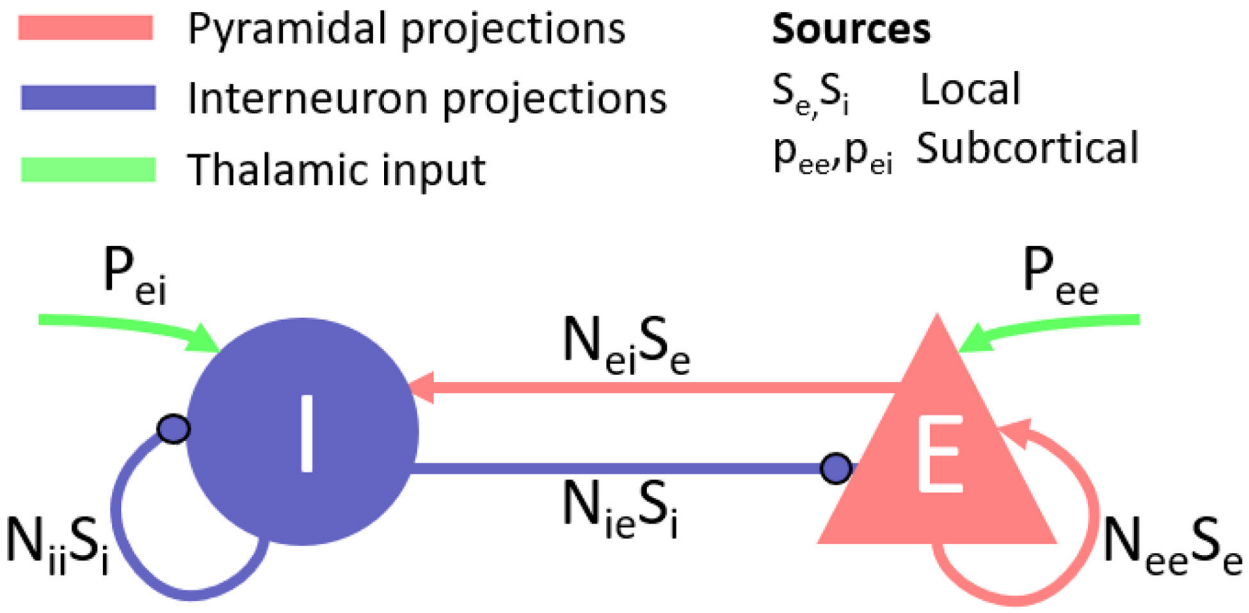

Figure 1:
Overview of neural mass model. *N* represents the number of synaptic connections. More information about the parameters is provided in Table A1.

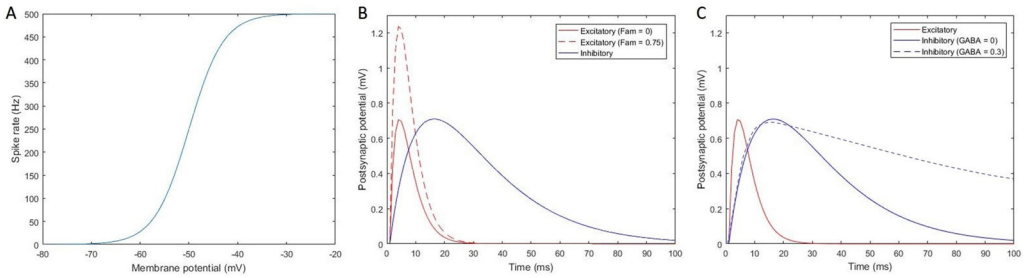

Figure 2:

A. Sigmoid activation function (excitatory and inhibitory) showing the influence of the membrane potential on mean neuronal firing rate (‘spike rate’). The other two figures show the synaptic response functions for excitatory and inhibitory synapses. The postsynaptic potential as a result of presynaptic input is shown on the y-axis. The baseline values are shown in both subplots. The effect of an increased amplification factor F_{am} on the synaptic response function is shown in 2B. The effect of an GABA-ergic drugs on the response function is visualized in 2C.

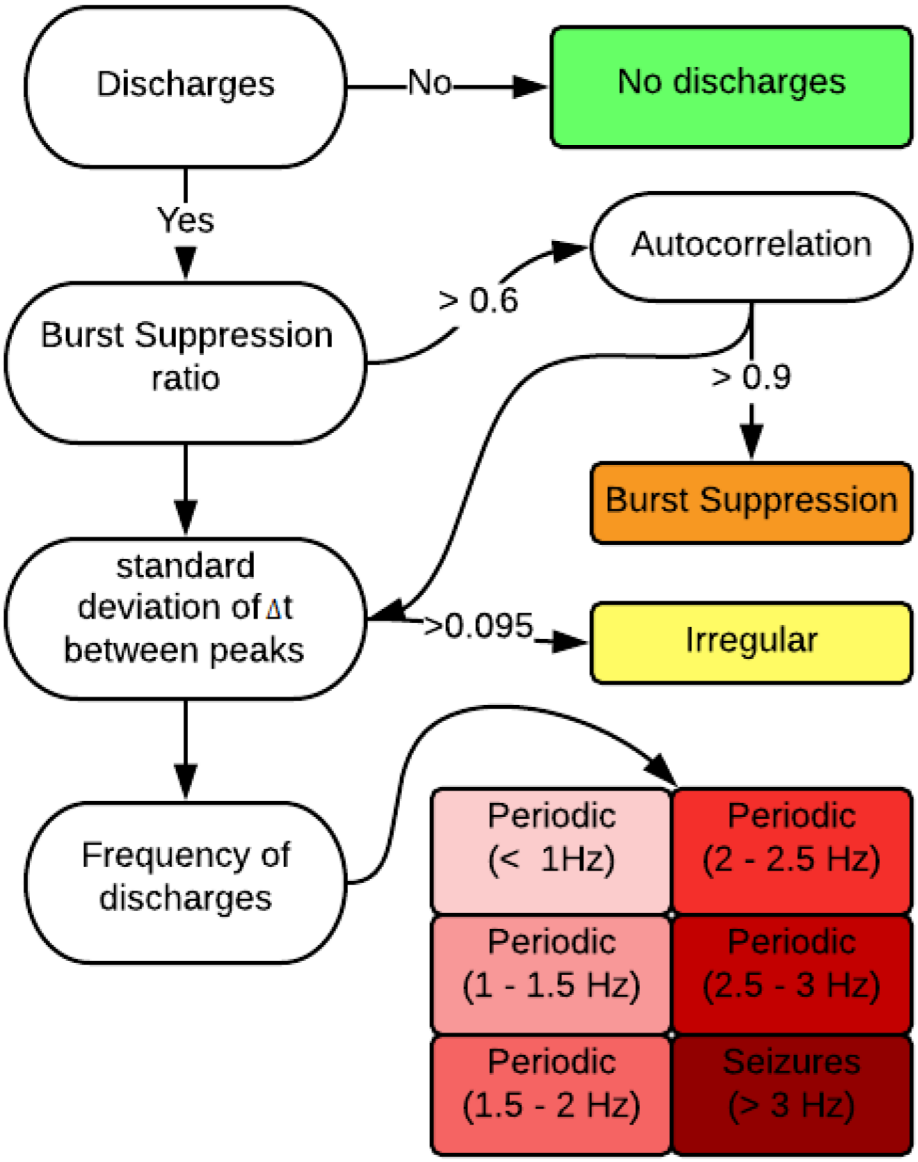

Figure 3:
Flowchart to categorize simulated EEG signals.

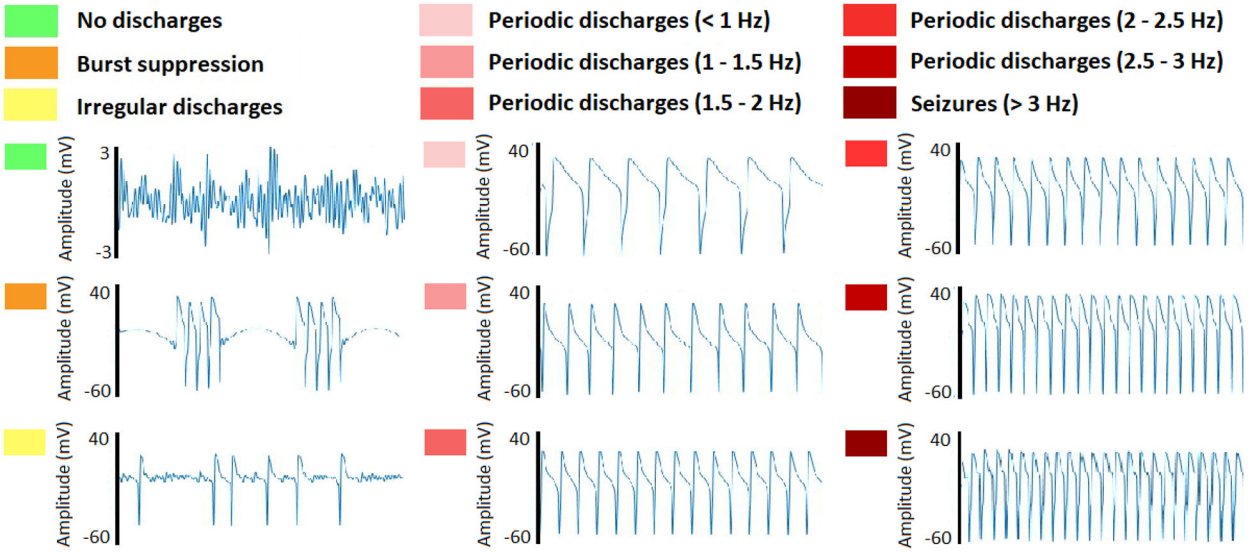

Figure 4:
Legend of Figures 5, 6, 7 and 8 and corresponding simulated EEG signals.

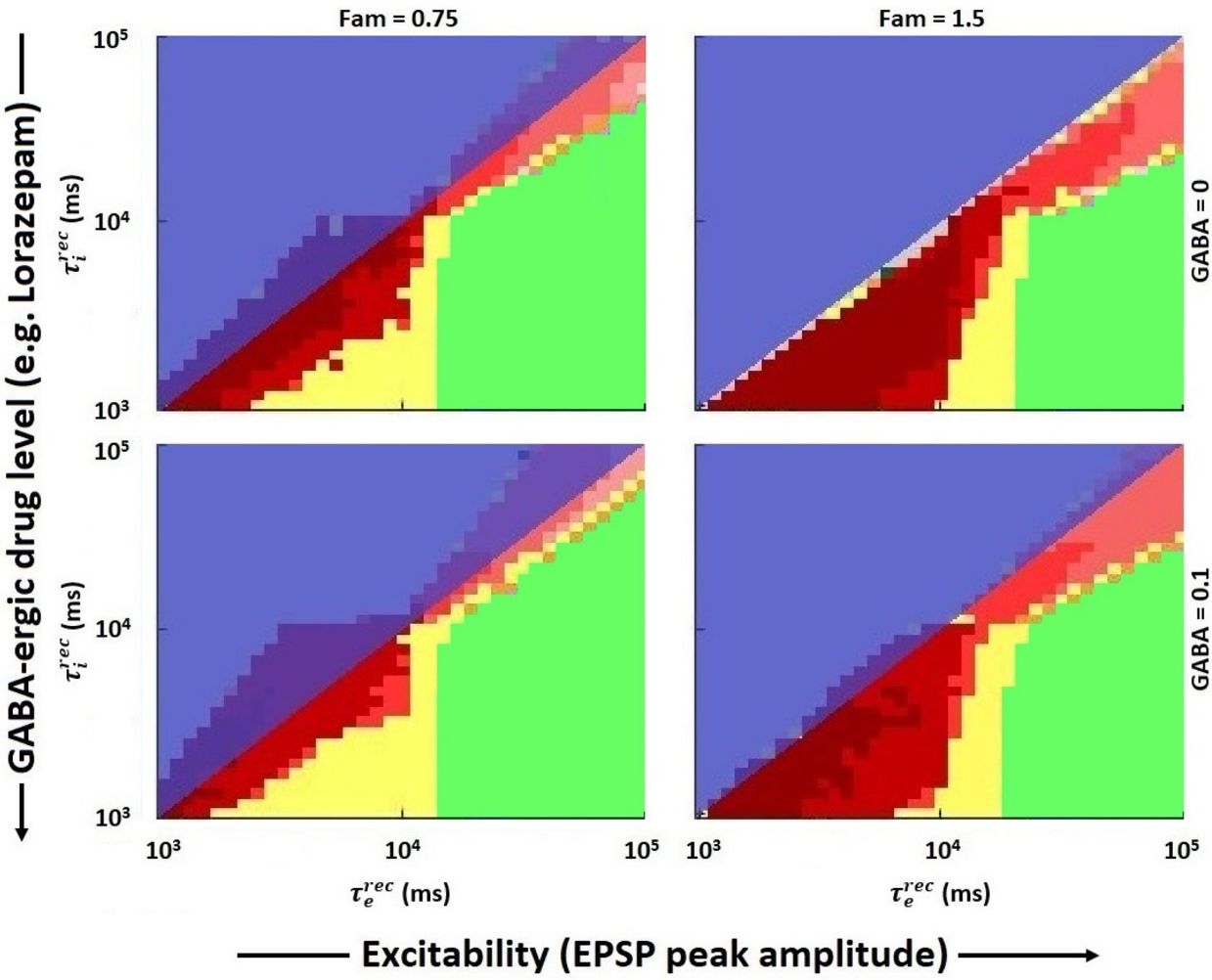

Figure 5:

Model behavior (see 4 for explanation of colors) as a function of the degree of elevated neuronal excitability (increased F_{am}), impaired synaptic neurotransmission (increased τ_i^{rec}, and τ_e^{rec}), and treatment (GABA-ergic drug level). Top two figures: GABA-ergic drug is absent; bottom two figures, GABA-ergic drug is present. Left two figures: lower level of neuronal excitability; right two figures: higher level of neuronal excitability. Each of the four figures shows model behavior (colors) as a function of the balance between the degree of impaired excitatory synaptic neurotransmission (excitatory EPSP recovery time constant (τ_e^{rec}; x-axis), and impaired inhibitory synaptic neurotransmission (inhibitory EPSP recovery time constant (τ_i^{rec}; y-axis). The shaded area masks the physiologically implausible region. EPSP: excitatory postsynaptic potential.

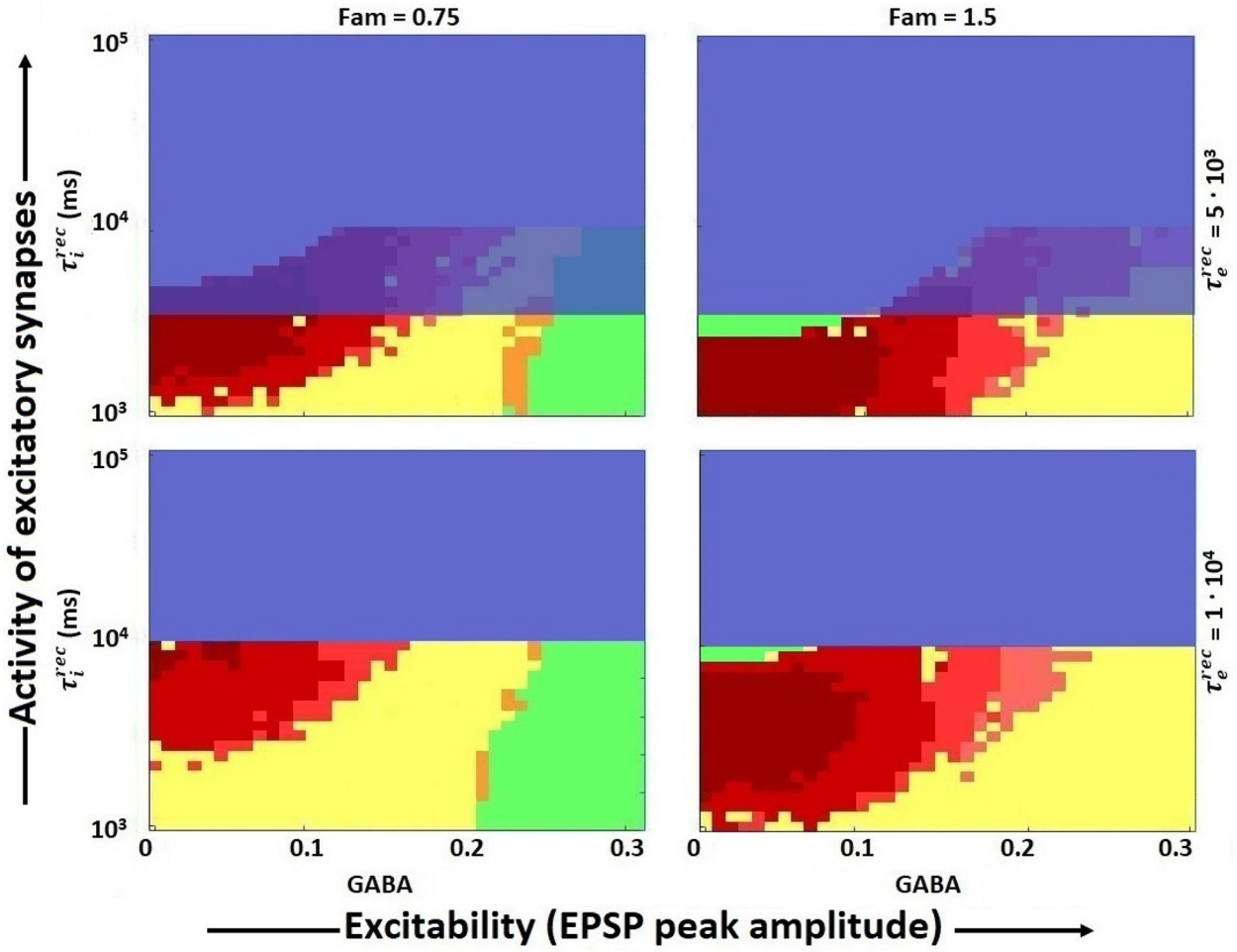

Figure 6:

Model behavior (see 4 for explanation of colors) as a function of the degree of elevated neuronal excitability (increased F_{am}), impaired synaptic neurotransmission (increased τ_i^{rec}, and τ_e^{rec}), and treatment (GABA-ergic drug level). Bottom two figures: higher impairment of excitatory neurotransmission; upper two figures: lower impairment of excitatory neurotransmission. Left two figures: lower level of neuronal excitability; right two figures: higher level of neuronal excitability. Each of the four figures shows model behavior (colors) as a function of the balance between the degree of impaired inhibitory synaptic neurotransmission (inhibitory EPSP recovery time constant (τ_i^{rec}; y-axis), and levels of GABA-ergic drug (x-axis). The shaded area masks the physiologically implausible region.

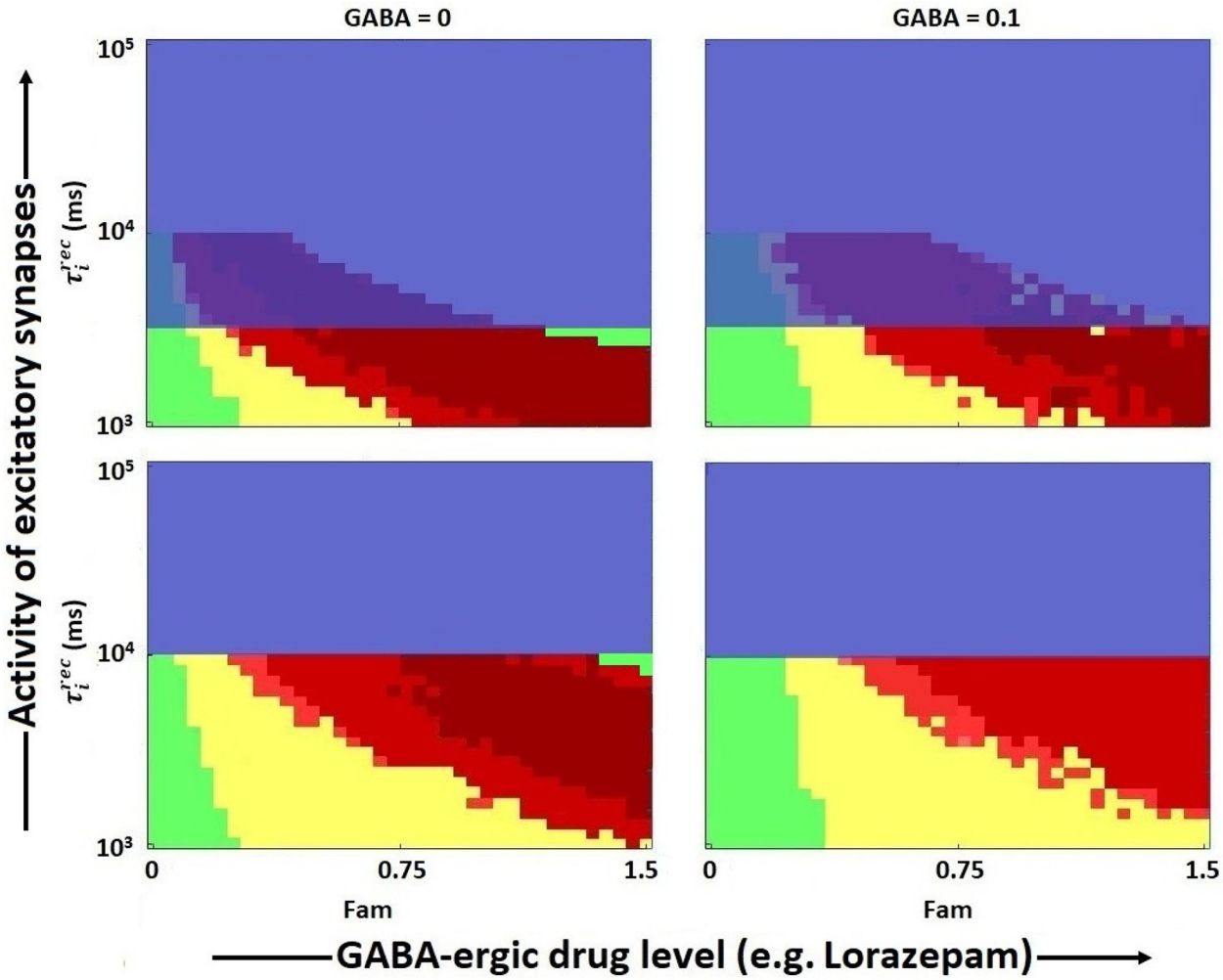

Figure 7:

Model behavior (see 4 for explanation of colors) as a function of the degree of elevated neuronal excitability (increased F_{am}), impaired synaptic neurotransmission (increased τ_i^{rec}, and τ_e^{rec}), and treatment (GABA-ergic drug level). Bottom two figures: higher impairment of excitatory neurotransmission; upper two figures: lower impairment of excitatory neurotransmission. Left two figures: GABA-ergic drug is absent; GABA-ergic drug is present. Each of the four figures shows model behavior as a function of the balance between the degree of impaired inhibitory synaptic neurotransmission (inhibitory EPSP recovery time constant (τ_i^{rec}; y-axis), and the degree of increased neuronal excitability (F_{am}; x-axis). The shaded area masks the physiologically implausible region.

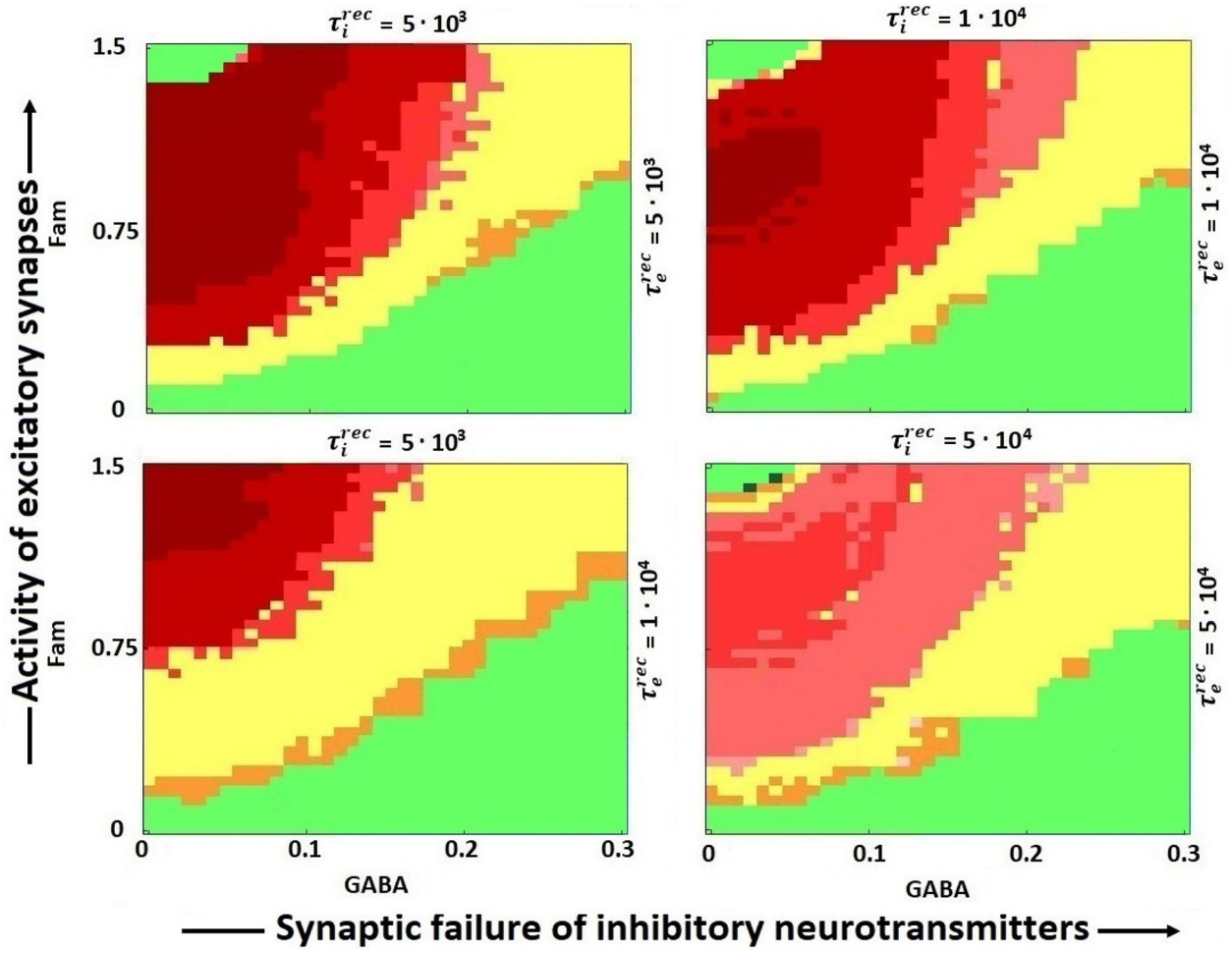

Figure 8:

Model behavior (see 4 for explanation of colors) as a function of the degree of elevated neuronal excitability (increased F_{am}), impaired synaptic neurotransmission (increased τ_i^{rec}, and τ_e^{rec}), and treatment (GABA-ergic drug level). Left two figures: less severely impaired inhibitory neurotransmission; right two figures: more severely impaired inhibitory synaptic neurotranmission. Bottom two figures: higher impairment of excitatory neurotransmission; upper two figures: lower impairment of excitatory neurotransmission. Each of the four figures shows model behavior (colors) as a function of the balance between the degree of increased excitability (F_{am}; y-axis) and the level of GABA-ergic drug (x-axis).

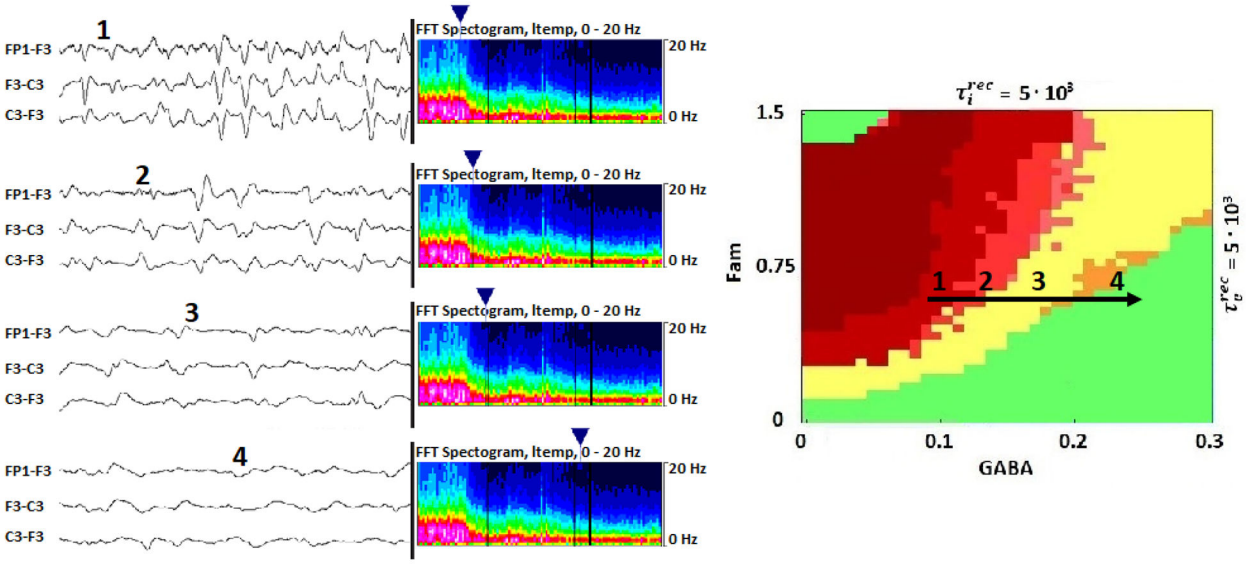

Figure 9:

Left: Raw EEG and accompanying spectrogram of a patient TME and GPDs, described in the electronic medical record as GPDs constituting NCSE before (1), and at various points in time after (2–4) administration of 2 mg of lorazepam. Triangles above the spectrograms indicate the time from at which the raw EEG is shown. We see that, following the bolus lorazepam, as CNS levels of the drug rise, the frequency of GPDs decreases, and finally they resolve. Right: The model exhibits the same qualitative behavior. The diagram shows the explanation of the observed changes in the EEG as predicted by the model, as GABA-ergic drug levels increase.

Table 1:

grades of Acute Hepatic Encephalopathy.

Grade	Signs	Changes on EEG
1	Confusion, reversed sleep-wake cycles, by mood changes, shortened attention span	Normal or suppressed alpha rhythm, diffuse beta activity
2	Mild disorientation, lethargy or apathy, inappropriate behavior, decreased inhibition	Abnormal. Loss of alpha rhythm, generalized theta slowing
3	Stuporous, obeys simple commands, gross disorientation	Abnormal. Generalized theta or delta slowing, GPDs (‘TPWs’) may occur
4	Coma, arousal to painful stimuli or not response.	Abnormal, very slow, high-amplitude theta-delta activity, GPDs (‘TPWs’) are common

Table 2:

Overview key parameters (default values)

τ_e^{rec}, τ_i^{rec}	$10^3 - 10^5$ ($\tau_e^{rec} > \tau_i^{rec}$)	Excitatory / inhibitory EPSP recovery time constants. ↑ values reflect impaired synaptic transmission
F_{am}	0–1.5	Amplification factor for peak EPSP amplitude. Increased value reflects increased neuronal excitability
GABA	0–0.3	Level of GABA-ergic drug (e.g. benzodiazepine).